Statistics of A-weighted road traffic noise levels in shielded urban areas

Statistics of A-weighted road traffic noise levels in shielded urban areas

Short title: Statistics of shielded road traffic noise levels

PACS: 43.28.Js, 43.50.Gf, 43.50.Lj, 43.50.Rq, 43.50.Vt

Jens Forssén and Maarten Hornikx
Applied Acoustics,
Chalmers University of Technology,
Göteborg, Sweden

Tel: +46 31 772 2200
E-mail address: jf@ta.chalmers.se

Abstract

In the context of community noise and its negative effects, the noise descriptors used are usually long-term equivalent levels and, sometimes, maximum levels. An improved description could be achieved by including the time variations of the noise. Here, the time variations of A-weighted road traffic noise levels have been studied. Of special interest are situations with a shielded courtyard. For numerical results, a ray model has been used for calculating the sound propagation, and the traffic has been modelled as a Poisson process. With this model the statistics of A-weighted levels have been investigated for different situations with varying traffic flows. Results from an in-situ measurement have been compared with those from the numerical model, showing acceptable agreement. It is shown both by numerical modelling and measurements that the time variations in noise level are smaller in a courtyard than in a corresponding directly exposed situation. One of the additional conclusions is that the noise reduction of the maximum level can be significantly higher than that of the equivalent level.

1 Introduction

The road traffic noise in urban areas has a large negative effect on health and wellbeing today. Possible strategies for improvement involve traffic planning, reduction of source strength by optimising tyre and road surface, noise barriers, tunnels, etc. In an ongoing project [1], effects are studied of planning buildings so that the inhabitants have access to a quieter side, for instance with a bedroom facing a shielded courtyard with much lower noise levels than outside the living room facing the street. It is known from previous research that, in many cases, the noise level in a courtyard is built up from multiple reflections and many sources within a large area [2]. This results in an acoustic situation that is different from that on the directly exposed side. With the tools available today, is it difficult to make a good noise level prediction for a courtyard situation. Therefore it is of interest to improve the modelling and understanding of such situations.

When studying the effects of traffic noise on annoyance, it is important to consider not only the long-term equivalent levels, but also the temporal variations of the noise levels (see e.g. [3]). The importance of the temporal variations has also been shown in sleep disturbance studies, where the maximum level is an important agent [4]. It should be noted that statistical treatment of road traffic noise is not a new topic within acoustics (see e.g. [5]). Possibly, the interest is renewed today after an intermediate period of extensive credit to long-term equivalent levels.

In this paper we have studied the temporal variations of road traffic noise for situations with a shielded courtyard and a directly exposed side. The traffic flow is modelled as a Poisson process, which is a model with a very low level of complexity compared with other microscopic traffic flow models. Less simplified models can involve car-following theories (see e.g. [6, 7, 8, 9]), which has previously been used also for noise predictions (see e.g. [10]). In a recent paper, a software based on car-following was used, and time variations of traffic noise were predicted for different positions within a large urban area [11]. The courtyard situation was not investigated, which is the main focus of the work presented here. The use of the Poisson model is motivated for situations when each vehicle can move with weak dependence on the other vehicles, for instance for low flow conditions [6]. The traffic model is further discussed in the next Section. In Refs. [12, 13], shielded environments as due to courtyards and balconies were studied, and statistics of noise levels due to traffic investigated. The conclusions drawn about the change in noise level variation, due to the shielding in a courtyard, is supported by the numerical and in-situ measured results presented here. Here, also time patterns are presented, as well as results for varying traffic flows.

A numerical ray model is used for calculating the sound propagation. The model is computationally fast, but the omission of higher-order diffraction leads to limited accuracy. More accurate models would presently be too time consuming, such as finite element or boundary element solutions of the Helmholtz equation, or by using more sophisticated diffraction calculations up to very high orders of reflection. The used ray model is validated by measurements in a scale model (see Appendix A). A numerical study is performed for different situations with varying traffic flows. The probability density functions (PDFs) of the A-weighted levels are investigated. Also, results from an in-situ measurement are compared with those from the numerical model.

2 Numerical study

2.1 Ray model

The ray model assumes that the sound propagates as a ray, rather than as a wave. As implemented here, the reflections in boundaries become rays in the specular direction. For vertical boundary surfaces, the amplitude reduction of the reflected ray is modelled by an absorption coefficient, here set to $\alpha = 0.05$ for all surfaces. For finite impedance ground surfaces, a spherical wave reflection factor is used [14]. Diffraction and diffusion effects may be modelled as add-on processes, as a consequence of the ray approach. Here, single edge diffraction is modelled for the rays that reach the courtyard. (A description of the used diffraction theory can be found in e.g. Ref. [15].) Curving of the rays, which would model refraction effects due to a vertical temperature gradient or wind, is not implemented. Also, scattering and decorrelation effects due to atmospheric turbulence are neglected here.

For free field propagation, a decay with distance as for spherical spreading is assumed. Additional decay due to air absorption is modelled following Ref. [16] with 70 % relative humidity, 10 °C temperature and standard atmospheric pressure. Reflections in vertical surfaces with a finite dimension are reduced in amplitude following the Fresnel zone model as described in Ref. [17], with an eighth of a wavelength as parameter value. The total number of reflections needed is found by studying the convergence of the resulting sound pressure level. For the situations investigated here, reflections up to order 64 have been included. Assuming acoustically hard vertical surfaces and no air absorption leads to only minor changes in the results. All reflections from one vehicle are added in phase, whereas contributions from different vehicles are added as uncorrelated contributions. Appendix A describes a validation of the ray model using scale model measurements.

The numerical study concerns simplified situations. In this Section all traffic is modelled as flowing on a single lane. In Section 3 a field situation is studied, resulting in a similar model but involving multiple lanes of traffic.

The geometry of the situation is shown in Figure 1. Parallel to the straight road is a 3 m high noise barrier, assumed to be thin and hard concerning the diffraction. A long building block is placed 15 m further away, also parallel to the road, thus forming a closed courtyard together with the barrier (closed in a two-dimensional sense). In the modelling the building is assumed to be infinitely high. The distance from the barrier to the closest vehicle wheels is taken as the source–barrier distance, 12 m. Between the barrier and the building, the receiver is located, at a distance of 7 m from the barrier, and at a height of 1.5 m. The ground surface is flat and acoustically hard. In Figure 1 also the coordinate system is shown, with the y-axis parallel to the road and the receiver at $y = 0$.

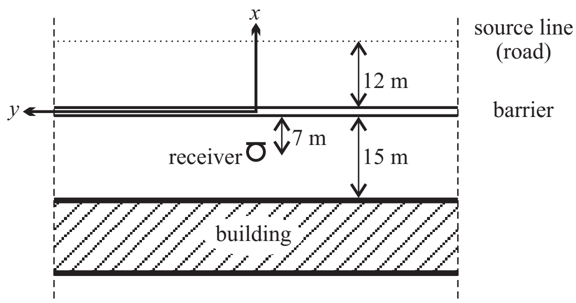

Figure 1: Geometry for the calculated situation.

The used source strengths are derived from the A-weighted equivalent levels given by the Nordic prediction model from 1996 [18]. The level for light vehicles is given for speeds above 40 km/h, at 10 m distance from the road and for one vehicle per second, as

$$L_{\mathrm{AEq,L}} = 73.5 + 25 \log 10(v/50), \tag{1}$$

where v is the vehicle speed (in km/h). For speeds above 50 km/h, the corresponding equation for heavy vehicles is

$$L_{\mathrm{AEq,H}} = 80.5 + 30 \log 10(v/50). \tag{2}$$

The source strengths include the reflection in the road surface, and assumes a source height of 0.5 m. However, in the study presented here the source is located on the ground surface. The cause for this is to better model the low location of the dominating source that is due to the tyre and road contact. Omni-directional sources are assumed. However, a test including directivity is made for the in-situ study. The source spectrum used here is taken from C_{tr}, the standardised third-octave band values from 50 to

5000 Hz for urban traffic noise [19]. The values are interpolated to a finer frequency resolution used in the calculations (20 components per third-octave band).

2.2 Traffic flow model

The vehicles are modelled as point sources with initially randomised positions according to a Poisson process. The distance ν between two consecutive vehicles is then an exponential random variable, with a PDF as

$$\frac{1}{\mu}\mathrm{e}^{-\frac{\nu}{\mu}}, \quad \nu \geq 0, \tag{3}$$

where μ is the mean distance between vehicles [6]. The exponential PDF has its largest value at zero distance, $\nu = 0$, which is unrealistic for traffic due to the length of the vehicles and a preferred minimum distance in between them. More realistic PDFs can involve a user-selected shift of the minimum time headway [6]. (The time headways can for instance be defined as the difference in time between passages of the vehicles' front wheels.) Here, however, the exponential PDF is used, as given by equation (3). As will be shown below, this can limit the acoustic modelling to cases where the contributions to the noise come from a road with many lanes.

Traffic data were collected by the Swedish Road Administration during one hour on a motorway with six lanes, where the speed limit was 70 km/h. The time between vehicle passages (time headway) is given for each lane with a precision of 0.01 s. As an example, the smoothed histogram for one of the lanes is shown in the inset in Figure 2 (bin size being 0.1 s). (All shown histograms are normalised to yield an estimate of the PDF, i.e. the PDF integrates to 1.) It can be seen that the agreement with the corresponding exponential PDF is poor at the shorter time headways. However, if the traffic on all lanes is seen as one process, a better agreement is reached. In this way, a passage on one lane can take place arbitrarily close in time to a passage on another lane. The non-smoothed histogram (bin size 0.01 s) for all lanes together and the corresponding exponential PDF are plotted in Figure 2. The agreement is good but one can discern a trend that the recorded data shows slightly lower probabilities at larger time headways, i.e. results in a slightly smaller standard deviation than the exponential PDF does. (The standard deviations are 0.45 and 0.57 s, respectively.)

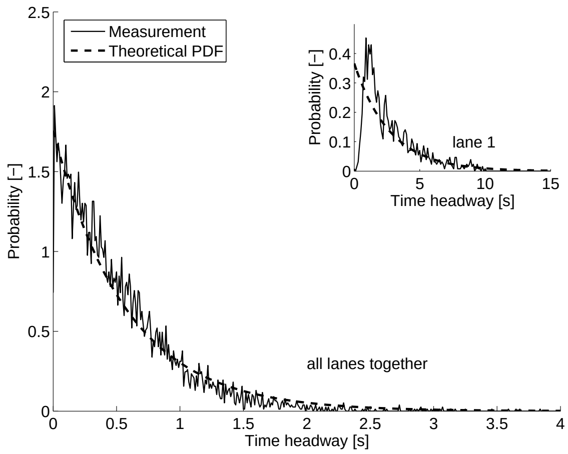

Figure 2: Histogram of measured time headways for the traffic on lane 1 (inset) and for all lanes together. The histograms are normalised to yield an estimate of the probability density function (PDF), i.e. sample probability. The theoretical exponential PDFs are also shown.

2.3 Pass-by patterns

After the initial vehicle positions have been randomised, the vehicles are moved along the road, in steps with length $v\Delta t$, where v is the speed of the vehicles and Δt is the time discretisation. Here the vehicle speed is $v =$70 km/h (19.4 ms^{-1}), and taken to be the same for all vehicles. The time discretisation, Δt, should be chosen short enough for a sufficient sampling of the time varying sound pressure level. Setting Δt as the time it takes for a vehicle to travel a quarter of the distance between the road and the receiver seems to be a good rule of thumb, and here a value slightly smaller than that has been used: $\Delta t = 0.22$ s. Numerical tests showed, for the situations studied here, negligible differences when the traffic was divided into two lanes with opposing flow directions, and both lanes still at the same distance from the receiver.

To speed up the calculations, pass-by patterns are pre-calculated, i.e. the time varying total A-weighted level as a vehicle moves from $y = 0$ to $y = y_{\text{max}}$, where $y_{\text{max}} = 2700$ m has been used here. (The values for $y \leq 0$ are given by symmetry.) In Figure 3 pass-by patterns are shown for the four different combinations of including or excluding the barrier and the building. The results are for a single heavy vehicle.

Comparing, in Figure 3, the two dashed curves, which show the results without the building, one can see that the relative effect of the barrier is reduced as the vehicle moves away from $y = 0$. The difference between a situation with and without barrier is about 16 dB at $y = 0$ and only about 3 dB at $y = 1000$ m. This behaviour is due to the smaller diffraction angle at larger y values, which corresponds to less screening effect. The results with the building show a similar but enhanced trend: the difference is about 14 dB at $y = 0$, whereas at around $y = 350$ m the curves cross. This means that a vehicle further down the road can be heard more easily if a barrier is placed between the road and the listener. The cause for this phenomenon is a combination of two different things going on. First, the diffraction angles get smaller for higher orders of reflection as well as for larger y values, which gives less screening effect. Second, when the reflection order is increased, the elongation of the propagation distance is shorter for large y values than for small y values. That is, for large y values, the low-order reflections are almost as strong as the zeroth order reflection. (The reflection order is the number of reflections in the building and the barrier together.) The second effect is displayed in Figure 4, where the propagation distance, r, is plotted as function of the reflection order, $N = 0 \ldots 64$. The six different graphs are for y values ranging from 0 to 1000 m in steps of 200 m, with the lowest graph for $y = 0$. It is apparent that the rate of increase of the propagation distance, r, when N increases from zero, is small for large y values and larger for small y values. Analytically, it can be shown that the rate of increase tends to zero as y tends to infinity. In other words, the contributions of the low-order reflections have about equal strength for large y values, whereas the strength decays rapidly with increased reflection order for y near zero. This results in a level as function of y which decays faster without the barrier than with the barrier.

A similar effect has been noted previously in a two-dimensional modelling of courtyards, which can be seen as a situation similar to the one studied here at $y = 0$ [20]. There it was concluded that multiply reflected contributions decay slower with increasing reflection order for far away roads than for roads nearby. This is due to that the change in propagation distance, when the reflection order is increased, is small compared with the total distance, if the road is far away in comparison with the size of the courtyard.

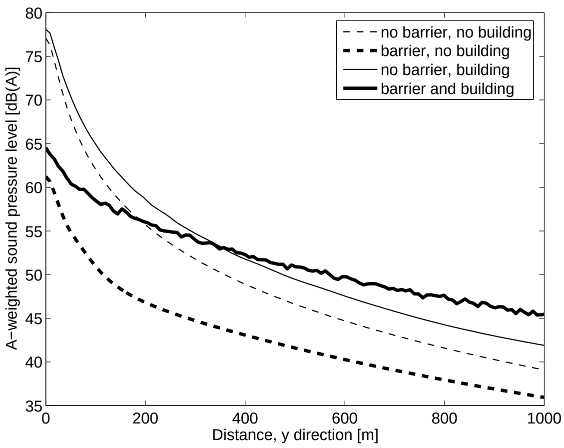

Figure 3: Pass-by patterns for the four different combinations of including or excluding the barrier and the building, for a heavy vehicle only.

The above explained phenomenon for the courtyard situation, i.e. the slow decay of a vehicle's noise contribution when y is increased, has strong implications on the resulting time variations of the levels, as will be shown below. The very strong effect of this phenomenon shown in Figure 3 is however assumed to have the possibility to

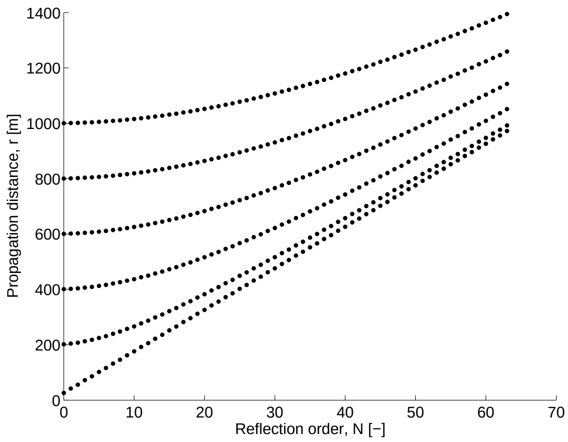

Figure 4: Propagation distance, r, plotted as function of the reflection order, $N = 0\dots64$. The six different graphs are for y values ranging from 0 to 1000 m in steps of 200 m, with the lowest graph for $y = 0$.

appear only when the vertical surfaces of the building and of the barrier give very small reflection losses.

2.4 Time patterns

An example of time patterns is shown in Figure 5 for the two cases with and without the barrier, both with the building. Here, the mean flow is 6250 vehicles per 24 hours (veh/24h) and 10 % are heavy vehicles. In the Figure, the heavy vehicles give rise to the three largest peaks of both curves. As discussed above, one can find situations where the level is higher with the barrier than without, here for instance at times around 65 s. The straight lines indicate the long-term equivalent levels, L_{Aeq}.

An important conclusion concerns the difference between the barrier's screening effect on the maximum level, L_{Amax}, and on the equivalent level. The peak level calculated here can be seen as an approximation of L_{Amax} since an integration time is used when measuring L_{Amax}. Looking at the peak levels the barrier gives a noise reduction of 13.5 dB. For the equivalent level, L_{Aeq}, the reduction is only 8.5 dB.

Hence, for the case studied here, the difference in screening effect amounts to 5 dB between peak and equivalent levels. (Since the same spectrum is used for heavy and light vehicles, the values of the noise reduction due to the barrier are independent of the vehicle type.) The explanation for this effect lies with the different pass-by patterns for the two situations: the courtyard situation (with the barrier and the building) and the directly exposed situation (without the barrier and with the building). The peak level is given at $y = 0$, and by comparing the courtyard situation and the directly exposed situation, the peak level can be seen to be reduced by about 13.5 dB (see the two solid curves in Figure 3). Due to the slower decay with distance, y, for the courtyard situation than for the directly exposed one, one gets a smaller difference between the equivalent levels (see Figure 3).

It should also be noted that the peak levels show very little variation in value, especially without the barrier. This is due to that, for the relatively low vehicle flow, there are seldom two vehicles close enough to significantly change the peak value of a vehicle pass-by. In addition, for these results, all vehicles are identical, except for the separation into light and heavy ones.

By introducing a random variation of the individual vehicles' source strengths, the time patterns become more realistic, as shown in Figure 6. The main assumption is that the level is normally distributed, as in the 1996 Nordic model [18]. However, the values of the corresponding standard deviations can today be concluded to be lower, see Ref. [21]. The same reference gives the following standard deviations: 1.4 dB for light vehicles at 90 km/h and 1.8 dB for heavy vehicles (≥ 3 axles) at 70 km/h. In the 1996 Nordic model the standard deviation is given by a factor times an exponential decrease with speed. Here, due to lack of further data, the same exponential decrease is assumed and only the factor is changed when applying the newer values from Ref. [21]. This leads to a standard deviation of 1.85 dB for light vehicles at 70 km/h.

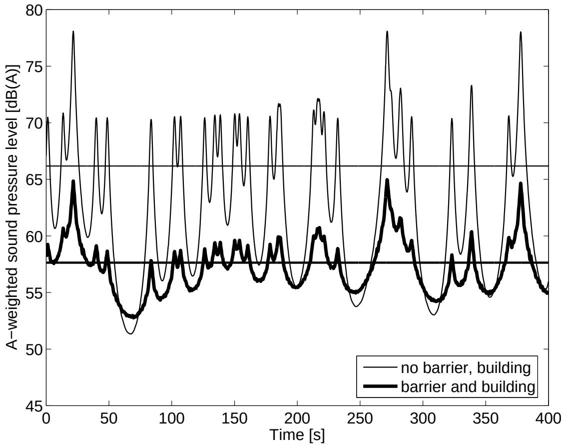

Figure 5: Example of time patterns for the two cases with and without the barrier, both with the building. The mean flow is 6250 veh/24h and 10 % are heavy vehicles. The straight lines correspond to long-term equivalent levels.

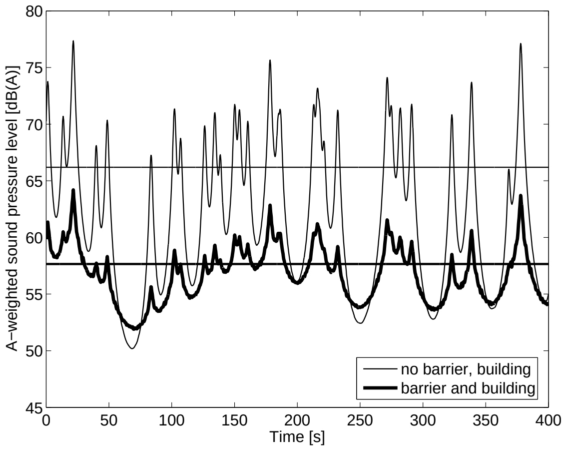

Figure 6: Example with randomised source strengths. Otherwise same conditions as for Figure 5.

2.5 Statistics of levels

Histograms of sound pressure levels have been calculated for the situation exemplified in Figure 6 and for other vehicle flows, including a randomised source strength as described above. The results in Figure 7 are for the directly exposed side (without the barrier and with the building), whereas Figure 8 shows the results for the courtyard (with the barrier and the building). The different histograms correspond to flows ranging from 1562.5 to 100000 veh/24h. The time length for the calculation of each histogram is chosen long enough to yield an estimated passage of 10000 vehicles.

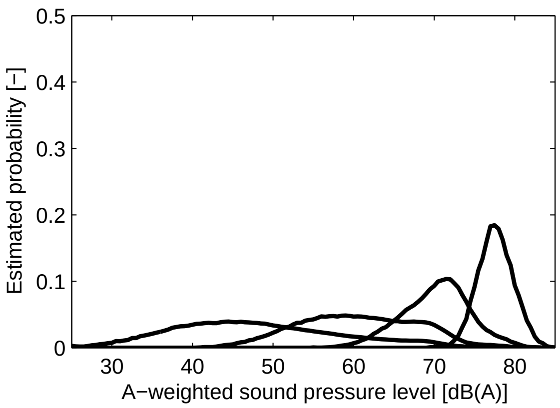

Figure 7: Histograms of the directly exposed levels for different traffic flows (1562.5, 6250, 25000, and 100000 veh/24h).

The histograms for the courtyard levels (Figure 8) show smaller spread than the respective histograms for the directly exposed levels (as has also been concluded in [12]). Also this effect is linked to the difference in pass-by patterns (see Figure 3). The slower decay with distance for the courtyard situation has the effect that, on average, a larger number of vehicles contribute to the received pressure, than for the directly exposed situation. When more vehicles are contributing, the standard deviation of the sound pressure level is reduced. (It could be noted that the standard deviation of a level in decibel shows similar qualities as the standard deviation of an acoustical power density normalised by its mean value.) Alternatively put, a slower decay with distance

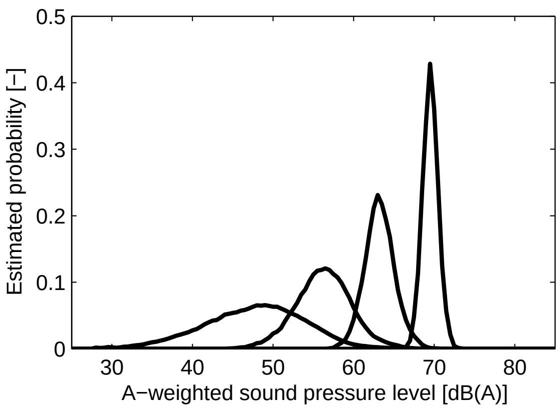

Figure 8: Histograms of the courtyard levels for different traffic flows (1562.5, 6250, 25000, and 100000 veh/24h).

(or vehicles contributing from a longer section of the road) causes less deep valleys between the peaks in the time patterns.

Some of the histograms have shapes far from Gaussian, especially on the directly exposed side and for the lower vehicle flows. The protrusions (bumps) shown at around 70 dB for these cases are given by the maximum levels of the light vehicles (Figure 7). Without the randomisation of the source strengths, peaks appear at around 70 and 78 dB, corresponding to the maximum levels caused by light and heavy vehicle, respectively. It should be noted that the modelling of the two different vehicle classes results in a much larger spread of sound levels, than if all traffic would consist of a single vehicle type, with averaged properties.

Table 1 displays the equivalent levels and the standard deviations (STDs) for the different flows, for the directly exposed side and for the courtyard. The maximum level, L_{Amax}, is independent of the flow. (For a single pass-by of a heavy vehicle the peak level is 78.1 dB(A) on the directly exposed side, and 64.5 dB(A) in the courtyard. The corresponding values for the light vehicles are 7.7 dB(A) lower.) The equivalent level, L_{Aeq}, increases with 3 dB for each doubling of flow. (It could be noted that, in practice, an increased flow would eventually lead to lower driving speeds.) In Figure 9 the standard deviations of the levels are plotted. They are higher in the directly exposed case than in the courtyard, as also stated above. The difference, in dB, between the STDs is large for the lower flows and decreases with increased flow. It can also be noted that, at the lower flows, the rate of decrease of the STDs with increased flow is about the same for the two cases.

Table 1: Levels and standard deviations (STD), for different flows.

Flow [veh/24h]	1562.5	3125	6250	12500	25000	50000	100000	200000
Directly exposed:								
$L_{\mathrm{Aeq}}[\mathrm{dB(A)}]$	60.2	63.2	66.2	69.2	72.2	75.2	78.2	81.3
STD [dB]	10.34	8.89	7.31	5.71	4.22	3.09	2.20	1.65
Courtyard:								
$L_{\mathrm{Aeq}}[\mathrm{dB(A)}]$	51.6	54.6	57.7	60.7	63.7	66.7	69.7	72.7
STD [dB]	6.20	4.63	3.44	2.56	1.86	1.41	0.96	0.75

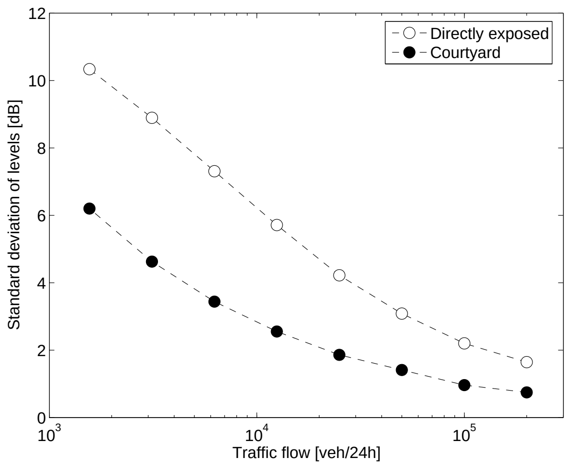

Figure 9: Standard deviation [dB] as function of traffic flow [veh/24h] for directly exposed side and courtyard.

3 Field measurement

3.1 Measurement conditions

The measurement site is a courtyard shielded from a nearby motorway by a noise barrier. The site was chosen because of the noise in the courtyard being dominantly caused by the traffic on the motorway, which simplifies the modelling. However, normally, in an urban area many roads must be taken into account for a good prediction of the noise level in a shielded courtyard.

Recordings were made during 45 minutes on two channels: one in the courtyard and one on the side of the barrier facing the traffic. All sections with audible anomalies were removed, resulting in 30 minutes of typical traffic noise. (Sections were removed which contained sounds of birds, doors, voices and similar, as well as untypical traffic sounds, such as from rattling metal parts, etc.)

The motorway has eight lanes as it passes the site. The lane closest to the courtyard is an exit lane and the lane furthest away is an entry lane. At the location where the traffic flow data were collected, the motorway has only six lanes. This is the same location as where the traffic data discussed in Section 2 were collected, and lies a few hundred meters away from the measurement site.

At the site, the barrier is only approximately parallel to the motorway; the angle between them being about $8°$. The building is U-shaped, thus forming an enclosed courtyard with a width of around 40 m in the y-direction. The shielding caused by the building is assumed to be partly compensated by the reflections in the corresponding facades. Hence, in the modelling a two-dimensional, parallel geometry is assumed (see Figure 10).

The source is taken to be located 1 m in on each lane, and at height $z = 0$. (In the

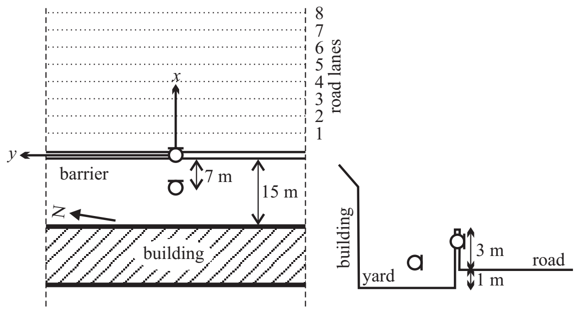

Figure 10: Geometrical model for the measurement site. Left: top view. Right: vertical section. The edges of the road lanes are at $x =$4.2, 9.0, 12.8, 16.6, 21.4, 25.2, 29.0 and 32.8 m.

caption of Figure 10 the distance to the edge of each lane is written.) At the edge of lane 2 and of lane 5 there is a low barrier, with a modelled height of 0.85 m. The effect of the low barriers on the noise in the courtyard is estimated to be negligible. However, on the face of the tall barrier, which has the receiver position 0.6 m below the barrier edge, the diffraction due to the low barriers is taken into account.

The tall noise barrier is made of wood, with a concrete fundament. The thickness of the barrier is 150 mm, but it is modelled as a thin, hard screen. The vertical surface of the building is mainly covered by wooden panels. In the courtyard the ground is dominantly grass covered. The ground impedance is taken from Ref. [22] as the two-parameter model for hard worn lawn, which in turn is used for calculating the spherical reflection factor. The ground plane of the courtyard is 1 m lower than the road plane. The microphone of the courtyard was placed 1.5 m above the ground plane. Outside the courtyard, a continuous asphalt surface is assumed even though there is a small strip of grass between the barrier and the road edge.

The measurements were made in the winter, on a Thursday afternoon (time 14:18–15:03). The temperature was $+4°$C and the relative humidity 87 %, which is used for the calculations below. The static pressure was 1027.8 hPa, the wind at 10 m height was around 5 m/s, from the south (i.e. a cross-wind situation), and the sky was partly cloud covered.

3.2 Comparison with calculations

The traffic data during the 45 minutes measurement was collected a few hundred meters to the north, along the same motorway. Unfortunately these data were not given at more detail than on one-minute intervals. Thereby we have less control of the time headway distributions than what is preferable. We do, however, assume that the more detailed data collected later are relevant, which are the data discussed in Section 2. (The data were collected on a Tuesday at around 14:00, with 152000 veh/24h, which gives similar traffic conditions as those during the noise measurements.)

The flow during the noise measurements was 161000 veh/24h, with 10.7 % heavy vehicles. The source spectra for light and heavy vehicles were taken from Ref. [23] as the Swedish data for 70 km/h (from categories *1a* and *3c+3d*, respectively). As previously, the total source strengths, in dB(A), were found from equations (1) and (2).

A bit south from the measurement site the motorway sloped upwards. By including this in the modelling, slightly higher noise levels were reached in the courtyard, whereas the levels on the directly exposed side were unchanged. (The up-slope started 50 m to the south and continued for 70 m with a constant slope, reaching 2.2 m elevation. Thereafter the motorway was flat.)

The calculations of the time patterns are made in a similar way as in Section 2, except for that described above, and that the different distances to the separate lanes is taken into account. The first lane (lane 1) has a lower flow rate (33 % of that on the other lanes) and a lower velocity (50 km/h instead of 70 km/h). This is taken into account in the modelling, except for the change in spectrum due to the lower speed, which is assumed to lead to negligible differences of the A-weighted levels.

In Figure 11, the equivalent levels as function of frequency are shown for the measurements and the calculations. One can see that the noise reduction is larger at the higher frequencies. The overall agreement between the measurements and the calculations is good, but there are some deviations. At lower frequencies the high measured levels could be due to that the motorway starts to slope upward near the site, which causes a heavier load on the vehicles and thereby more noise from the power train, which is not modelled here. The peak near 80 Hz is assumed to be due to engine noise, related to the ignition cycle. Most vehicles had studded tyres, which leads to the increased level shown at around 5–8 kHz. However, a more general increase due to the studded tyres was expected. In the courtyard, at higher frequencies, the relatively strong measured levels could be due to diffusion effects. That is, the stronger sound reaching higher positions on the building are scattered in non-specular directions within a broad angle, thereby increasing the sound level in the shadow region formed by the barrier. Possibly, also scattering due to turbulence could cause a similar increase at high frequencies. Since the focus here is on A-weighted levels, no further attempt has been made of improving the spectral agreement.

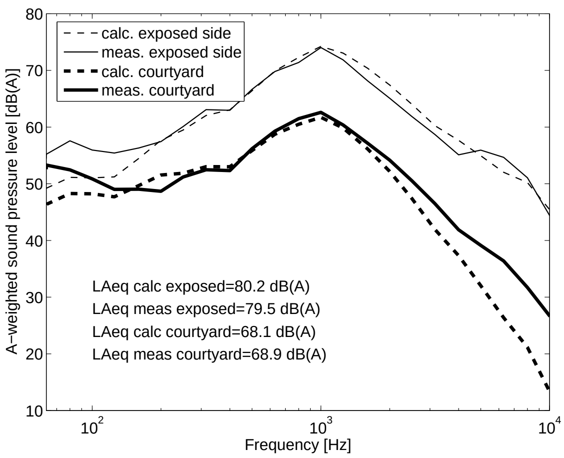

Figure 11: Measured and calculated third-octave band levels (A-weighted) for the directly exposed side and the courtyard.

The measured L_{Aeq} is 79.5 dB(A) on the directly exposed side and 68.9 dB(A) on the courtyard. The deviation of the calculated levels is less than 1 dB. Possibly, errors due to different approximations and assumptions partly cancel in the calculated results. For instance, the used source power data (equations 1 and 2) are stronger than the ones given by Ref. [23], which could counteract the expected increase due to the studded tyres, as well as the expected increase in tyre-road noise due to the low outdoor temperature. In addition, the front level is very sensitive to the exact height and position of the low barriers on lanes 2 and 5. This problem could be circumvented by using multiple source heights for each vehicle, as is planned in the new prediction methods under development [23, 24], where also source directivity is modelled. A test was made where a source directivity was modelled. For this test the directivity according to Ref. [23] was used. The most prominent feature of the directivity is that it shows a dip sideways to the vehicle, thus reducing the level when the vehicle is closest to the receiver. Concerning the calculated results, the inclusion of directivity caused a slight increase in the courtyard level (of 0.7 dB(A)), and a negligible change on the front side. (Concerning noise imission predictions, it could be noted that no correction to free field conditions has been made here, which would result in a 6 dB lower level on the directly exposed side. Moreover, when predicting the equivalent levels over 24 hours, they are expected to be about 2 dB lower than the daytime levels measured here.)

The contributions from the different lanes to the equivalent level range from 61 to 76 dB(A) on the directly exposed side. On the courtyard, the contribution from lane 1 is 49 dB(A), whereas the other lanes contribute with larger values, within a very small range of 59.2–59.8 dB(A). Thereby it can be assumed, at least for the courtyard calculations, that the multi-lane assumption is valid, which is used for being able to apply the exponential distribution for the time headways.

An excerpt of the measurement is shown to the left in Figure 12, and an example of a calculated time pattern is shown to the right. The time steps are 0.19 s for the measurements and 0.17 s for the calculations. For both sides more fine-structure variations are shown by the measured signals. On the front side the measured and the calculated time patterns seem to have a similar behaviour, except that a slightly larger spread can be seen in the calculations (see also Figure 13). The test made where source directivity was included, as described above, led to a better agreement for the front side results, concerning the corresponding histograms. For future work it would be of interest to implement the more complex directivity according to Ref. [24]. For the yard side, the patterns look more different. The calculations show smaller variations than the measurements (see also Figure 13). Possibly this could be due to that the building at the measurement site is U-shaped, and formes an enclosed yard. The test where directivity was included did not lead to any improvement of the courtyard results.

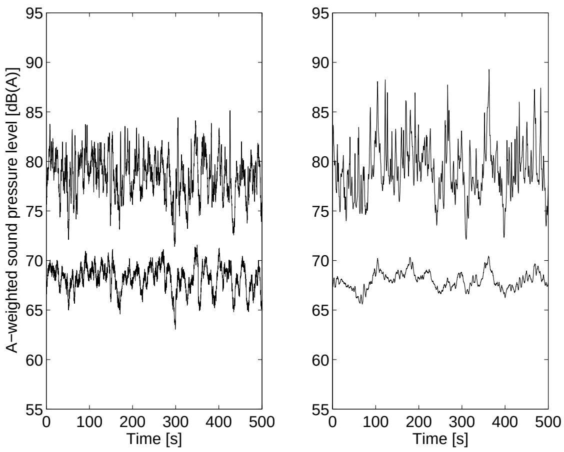

Figure 12: Examples of time patterns: Measured to the left and calculated to the right. Higher curves for the directly exposed side; lower curves for the courtyard.

The calculated histograms from modelling and measurements are shown in Figure 13 (bin size 1 dB), where also the corresponding standard deviations are displayed. As expected, the standard deviation is much larger on the front side than in the courtyard, as is shown by both the measurements and the modelling.

The difference between the modelling and the measurements does however look significant. Some possible errors have been discussed above, but all causes for the

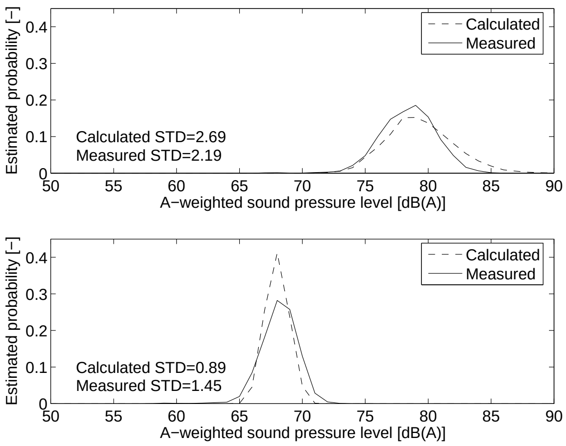

Figure 13: Predicted and measured histograms of A-weighted noise levels. Top: Directly exposed side. Bottom: Courtyard.

differences are not understood at present. In order to reach an improved agreement and understanding, several different sites need to be investigated in a similar way. Thereby a refinement of the modelling could be enabled, as well as a better idea of what level of agreement of the histograms can be expected for this kind of situations.

4 Discussion and Conclusions

Time variations of A-weighted traffic noise levels have been studied for shielded and directly exposed situations. The used numerical ray model has been validated by measurements in a scale model. Also, results from an in-situ measurement have been compared with those from the numerical model. A numerical parameter study has been performed, where statistics of A-weighted levels are investigated for situations with varying traffic flows, using a Poisson model for the traffic. It should be noted that for predictions of a larger variation of situations than studied here, more advanced traffic flow models would be useful, which can incorporate more detailed conditions, for instance individual vehicle speeds. However, it was concluded here that for a larger number of lanes, the total flow can be well approximated by a Poisson model.

The shielded situation of main focus is a courtyard created by a noise barrier in parallel to a building, and with a road outside and parallel to the noise barrier. Due to multiple reflections between the building and the barrier, the noise from a vehicle may decay very slowly with distance, as compared with the case without barrier, i.e. a directly exposed case. This effect has large implications on the traffic noise. One implication is that a vehicle further down the road can be heard more easily if a barrier is placed between the road and the listener.

Another implication concerns the difference between a barrier's noise reduction of the maximum level and of the equivalent level. In the numerical study of the courtyard situation, the noise reduction of the peak level was 5 dB higher than the noise reduction of the equivalent level.

The probability density functions (PDFs), or histograms, for the courtyard levels show a smaller spread than the respective PDFs for the directly exposed levels (as has also been concluded in [12]). Also this is due to the slower decay with distance for the courtyard situation. The cause is that, on average, a larger number of vehicles contribute to the received pressure in the courtyard, than for the directly exposed situation. When more vehicles are contributing, the standard deviation of the sound pressure level is reduced. Alternatively, this can be understood from that the slower decay with distance causes the time-varying level to have less deep valleys between the peaks. Predictions of the PDFs can be used for instance for an estimation of the proportion of time during which the noise level does not exceed some chosen value.

When comparing the results measured in situ with the calculated ones, the time variations of the levels look fairly similar. However, on the directly exposed side, larger variations are shown by the calculations than by the measurements. For the courtyard results, the opposite is shown, i.e. that the measured level varies more over time than the calculated one. These differences are also shown by the PDFs. The agreement between the predicted and the measured PDFs is acceptable in the sense that the predictions can clearly discern between a courtyard situation and a directly exposed one. The differences between the PDFs do however look significant. The reasons for the differences are not wholly understood at present. When a source directivity was included, a better agreement was attained for the directly exposed side. The courtyard results were however not improved. Possibly, one significant source of error could be that the courtyard modelling assumes a two-dimensional, parallel geometry instead of a U-shape. In order to reach an improved agreement and understanding, several different sites need to be investigated in a similar way. Thereby a refinement of the modelling could be enabled, as well as a better idea of what level of agreement of the PDFs can be expected for this kind of situations.

It should be noted that modelling different vehicle types is needed for good predictions. An improvement could probably be reached by using more than the two types used here, i.e. light and heavy vehicles. For future work it could also be of interest to study the (super) spectra of the level fluctuations in shielded areas, similarly to what has been done for directly exposed cases in Refs. [25, 11]. This could provide an additional link to annoyance. Moreover, it would be of interest to investigate the effects on annoyance of the fact that the sound in shielded areas is relatively stronger at low frequencies than the sound in directly exposed areas. In addition, considering the time signals of the sound pressure in courtyard situations, the prolongation of the impulse response due to diffraction and reflections may also change the perceived noise situation.

Acknowledgments

For the traffic data we are thankful to Joakim Elfving at the Swedish Road Administration. We would also like to thank Gunnar Lannér and Ulf Sandberg for valuable input. The work behind this paper has been funded by the Swedish Foundation for Strategic Environmental Research (MISTRA).

Appendix A. Scale model measurements – validation of the ray model

To validate the numerical ray model used in the paper, scale model measurements were executed. A 1 to 40 scale model was built in the anechoic room at Applied Acoustics, Chalmers University of Technology. The frequency range was limited to 4 kHz–45 kHz, corresponding to full scale third octave bands from 100 Hz up to 1 kHz. The dimensions and frequencies that are used below represent the full-scale situations.

Figures 14 and 15 show a picture and a vertical cross section of the scale model setup. The used materials were chosen to yield a specular reflection and to have a low absorption coefficient ($\alpha < 0.05$) in the relevant frequency range. For the ground, a chipboard plate coated with a thin layer of melamine (a plastic) was used. The barrier was made of plywood, and its top was made narrower to approximate a thin barrier. The width of the barrier top was 120 mm, which is less than half a wavelength at the highest frequency. The building row, 20 m high and 100 m long, consisted of cubic boxes of plexiglass (acrylic glass). The building and barrier row were terminated by absorption material to minimize unwanted end-effects.

In the model measurements, the source position was fixed whereas the microphone position was changed along the y direction (parallel to the barrier). The microphone height was 0.39 m. Note that the reciprocity principle was used; the source and microphone position were interchanged from their actual positions. The MLS technique was used to obtain the impulse responses. A tweeter source was chosen with a response in the above mentioned frequency range (Thiel and Partner, type $C^2$12-6). To obtain an omni-directional source, the tweeter was placed below the ground level, covered by a thin plexiglass plate with a circular hole. The size of the hole was designed to approximate an omni-directional field. An 1/8 inch condenser microphone, type B&K 4138, was used as the receiver. The microphone has a flat frequency response but has some directionality effects increasing with frequency. The influence of these effects was not relevant for the chosen microphone positions.

An effect that has to be paid attention to in scale modelling is excess air attenuation caused by a frequency dependent damping of sound waves in air. The excess attenuation is stronger for the higher frequencies and determines an upper frequency limit of scale model study measurements. The excess attenuation has to be corrected for before a comparison with model calculations is made. Since air damping is (travel) time and frequency dependent, a correction in either time or frequency domain will not be correct. Here, a correction using the continuous wavelet transform has been used (see e.g. [26, 27]). The wavelet transformed impulse response signal is localized in both time and frequency. A Morlet mother wavelet, order 20, was chosen. The transformed signal is corrected for excess attenuation in the two dimensional field (related to time and frequency) and an inverse transform returns the corrected signal. Since the wavelet transformed signal is localized in both time and frequency, the use of a wavelet transform seems a natural choice for correction of excess air attenuation. Among existing ways of correcting are those involving a short-time Fourier transform or narrow-band filtering of the time signal (see e.g. [28, 29]).

Figures 16–19 show a comparison between measured and calculated sound pressure levels (SPL), plotted relative to the free field level for a receiver at $y = 0$. The calculations are made using the ray model as described in the paper. The top panels show narrow-band results and the bottom panels third octave band results. The figures are for the two situations with a barrier only, and with a barrier and a building row. For each of these situations there are two y positions: $y = 0$ and $y = 80$ m. In general, a good agreement was found. The interference dips at 800 Hz in figures 16 and 18 are more pronounced in the calculations than in the measurements. This can be attributed to diffusive effects caused by small gaps between the plexiglass boxes and diffraction by the building top; no diffusive effects have been included in the numerical modeling.

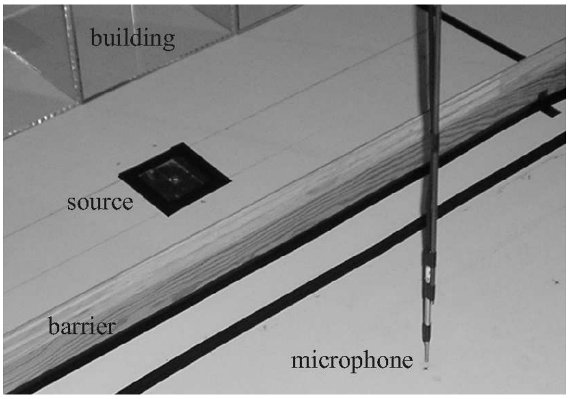

Figure 14: Picture of the setup for the scale model measurements.

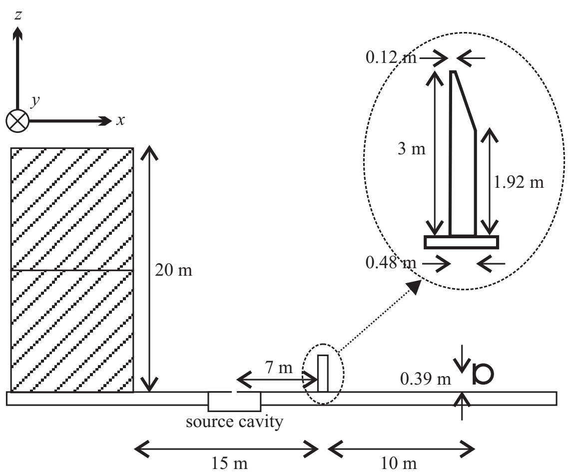

Figure 15: Geometry of the setup for the scale model measurements.

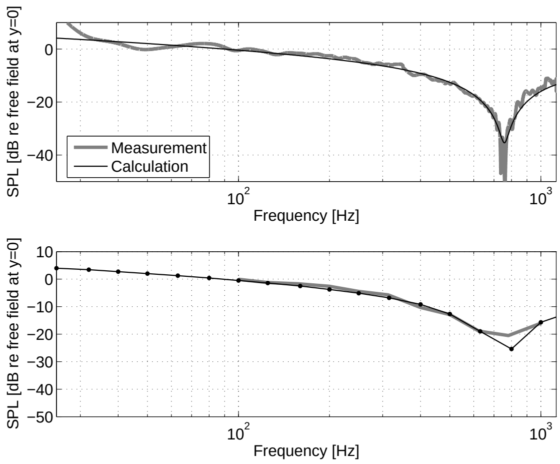

Figure 16: Comparison between measured and calculated levels for $y = 0$, with barrier only, i.e. no building row. The top panel shows narrow-band results and the bottom panel third octave band results.

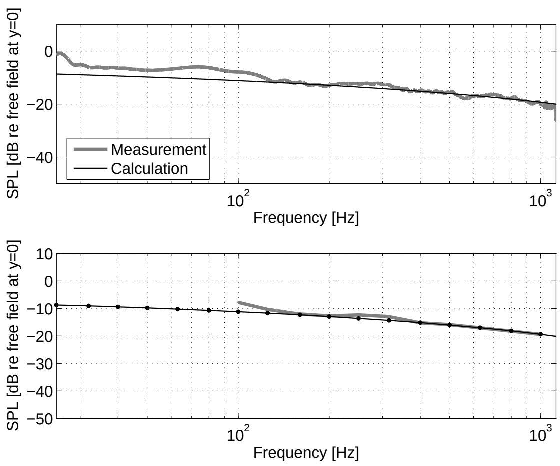

Figure 17: Same case as in Figure 16 except for y changed to 80 m.

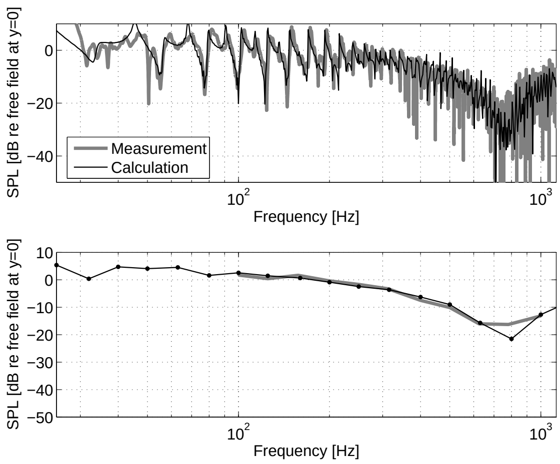

Figure 18: Comparison between measured and calculated levels for $y = 0$, with barrier and building row. The top panel shows narrow-band results and the bottom panel third octave band results.

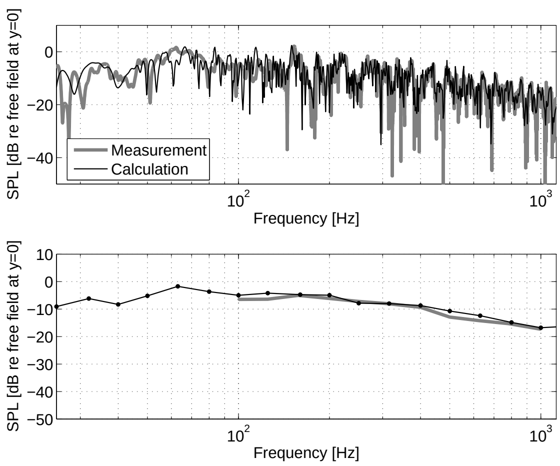

Figure 19: Same case as in Figure 18 except for y changed to 80 m.

References

[1] Soundscape Support to Health (www.soundscape.nu).

[2] Ögren M and Kropp W. Road Traffic Noise Propagation between Two Dimensional City Canyons using an Equivalent Sources Approach. Acustica–Acta Acustica, Vol. 90, 2004, pp. 293300.

[3] Roberts, M. J., Western A. W. and Webber M. J. A theory of patterns of passby noise. J Sound Vibr, 2003, Vol. 262, pp. 10471056.

[4] Öhrström, E. Effects of low levels of road traffic noise during the night: a laboratory study on number of events, maximum noise levels and noise sensitivity. J Sound Vibr, 1995, Vol. 179, pp. 603615.

[5] Griffiths, I. D. and Langdon, F. J. Subjective response to road traffic noise. J Sound Vibr, 1968, Vol. 8, pp. 16-32.

[6] May, A. D. Traffic flow fundamentals. Prentice Hall, New Jersey, 1990.

[7] Highway Capacity Manual 2000; Metric Version Transportation Research Board ISBN: 0-309-06681-6.

[8] Nagel, K. and Schreckenberg, M. A cellular automaton model for freeway traffic. J Phys I Fr 1992;2(12), pp. 2221-2229.

[9] Mason, A. D. and Woods, A.W. Car-following model of multispecies systems of road traffic. Phys. Rev. E 55 (1997), pp. 2203-2214.

[10] Jones, R. R. K. , Hothersall, D. C., and Salter, R. J. Techniques for the investigation of road traffic noise in regions of restricted flow by the use of digital computer simulation methods. J Sound Vibr, 1981, Vol. 75, pp. 307-322.

[11] De Coensel, B., De Muer, T., Yperman, I., and Botteldooren, D. The influence of traffic flow dynamics on urban soundscapes. Applied Acoustics, Vol. 66(2), 2005, pp. 175-194.

[12] Oldham, D. J., Mohsen, E. A. A model investigation of the acoustical performance of courtyard houses with respect to noise from road traffic. Applied Acoustics, Vol. 12(3), 1979, pp. 215-230.

[13] Oldham, D. J., Mohsen, E. A. The acoustical performance of self-protecting buildings. Journal of Sound and Vibration, Vol. 65, 1979, pp. 557-581.

[14] Chien, C. F. and Soroka, W. W. Sound propagation along an impedance plane Journal of Sound and Vibration, Vol. 43, 1975, pp. 9-20.

[15] Rasmussen, K. B. Model experiments related to outdoor propagation over an earth berm. J. Acoust. Soc. Am., Vol. 96, 1994, pp. 3617-3620.

[16] Acoustics – Attenuation of sound during propagation outdoors – Part 1: Calculation of the absorption of sound by the atmosphere. ISO 9613-1:1993, The International Organization for Standardization, 1993.

[17] Plovsing B. and Kragh J. Nord2000. Comprehensive Outdoor Sound Propagation Model. Part 1: Propagation in an Atmosphere without Significant Refraction. Delta report AV 1849/00, Lyngy, Denmark, 2000.

[18] Road Traffic Noise - Nordic Prediction Method. TemaNord 1996:525, Nordic Council of Ministers.

[19] Acoustics – rating of sound insulation in buildings and of building elements – part 1: Airborne sound insulation. ISO 717-1:1996, The International Organization for Standardization, 1996.

[20] Ögren, M. and Forssén J. Prediction of noise levels in shielded urban areas. Proc. Inter-Noise 2001, Hague, Holland.

[21] Sandberg, U. Noise emissions of road vehicles – Effect of regulations. Final report. International Institute of Noise Control Engineering, 2001.

[22] Attenborough, K. Ground parameter information for propagation modeling. J. Acoust. Soc. Am., Vol. 92, 1992, pp. 418-427.

[23] Jonasson H. G. and Storeheier S. Nord 2000. New Nordic prediction method for road traffic noise. Technical Report 2001:10, SP Swedish National Testing and Research Institute; 2001.

[24] Engineering method for road traffic and railway noise after validation and fine-tuning. Technical Report HAR32TR-040922-DGMR20, Harmonoise WP 3.

[25] De Coensel B., Botteldooren D., and De Muer T. 1/f noise in rural and urban soundscapes. Acustica–Acta Acustica, Vol. 89, 2003, pp. 287295.

[26] Torrence, C. and Compo, G.P. A practical guide to wavelet analysis. Bulletin of the American Meteorological Society, 1998, pp. 61-78.

[27] Daubechies, I. Ten Lectures on Wavelets. Society for Industrial and Applied Mathematics, Philadelphia, 1990.

[28] Picaut, J. and Simon, L. A scale model study experiment for the study of sound propagation in urban areas, Applied Acoustics 62, 2001, pp. 327-340.

[29] Akil, H. A. and Oldham, D. J. Digital correction for excessive air absorption in acoustic scale models. Proc. of the Institute of Acoustics, Acoustics 94, 1994, Salford, 16(2), pp. 525-536.